

# Dynamic Modelling of Fluid Interactions for Typical Sports Utilities

Rajesh Kumar<sup>1</sup>, Jyotirmoy Ray<sup>2</sup> and Subir Kumar Saha<sup>1</sup>

<sup>1</sup>*Mechanical Engineering Department, Indian Institute of Technology Delhi*

<sup>2</sup>*Wipro Infrastructure Engineering*

*ABSTRACT — Differentially shaped balls and objects are a characteristic of many outdoor games. The environment and corresponding fluid (air) interaction plays a vital role in the motion of the objects. This paper presents a method combining Screw Theory and Finite Element Theory to model the fluid interactions on rigid bodies. The method evades the use of different dynamics' equations and different force models for different objects. The methodology considers the application of local wrenches and their combined reduction to a specific coordinate. The framework is hence, independent of the type of object considered. The formalism developed is experimentally tested for a frisbee and proved using existent experimental results for a rugby ball, tennis ball and a football.*

## 1 Introduction

Dynamics of the rigid bodies allows prediction of motion of the object and has been of vital utility over the years. In the field of sports as well, the requirement of dynamics has been observed. Many of the sports include motion of objects in space. The sports include cricket, disc-throw, soccer, rugby etc. Analysis of motion of such objects has incredible implications on the development of sports equipments as well as leads to the improvement of the sports. Considering the “*outdoor ball games*”, the motion of the ball is heavily dependent on the environmental conditions. The fluid interaction on the ball considerably affects the motion. The fluid interaction methodologies usually require formulations of differential equations based on the shape of the object.

This paper proposes a methodology to predict the motion of an arbitrary shaped body moving under non-vacuum conditions. A combination of the finite element method and screw theory is used to model the solid-fluid interaction to understand the behavior of a rigid body. Differently shaped bodies have been analysed under non-vacuum conditions. The objects used in sports have been under consideration of the researchers over the decades [1-5]. The objects like football, rugby ball, tennis ball, cricket ball etc have been studied in detail. The method is developed for two separate systems – one with surface quadrilateral elements and the other with four sided prismatic elements. The methodology allows generalizing the forces on the elements rather than using different fluid force variations for different geometries. The developed method allows us to locally calculate the wrench on each element rather than the complete body. So, the parameters for a given environment needs to be determined only once and can be extended to any shape and size of rigid bodies following the given particular structure. The methodology was tested against experimental results for the sports utility objects like the Frisbee, football, tennis ball, and a rugby ball. The methodology developed does not require the determination of the secondary coefficients like the pitch moment coefficient and the roll moment coefficient [1].

## 2 Basis of the Methodology

The fluid-rigid body interaction, in the available literature [1] is heavily dependent on development of differential equations and providing formulations of their quick solutions. The various force-moment coefficients are usually required to be calculated in order to formulate the problem. The methodology developed divides the force acting on an object into two categories – the primary fluid forces and the secondary fluid forces. The primary fluid forces

acting on the rigid body are those that are known to affect the instantaneous area of contact of the fluid with the object. This means that the dissipative forces like the drag force depends on the relative velocity of the patch of interaction with the fluid, hence doesn't require the model of the whole object in space. The secondary forces constitute the body forces acting on the fluid, such forces affect the motion of the object due to the properties of the rigid body motion itself, like the magnus force [2]. The magnus force implicitly depends on the angular velocity of the object and acts along the surface of the object. The characterization of the surface of the object has also been given due importance.

The rigid body under analysis is either discretised into four-sided prismatic element or a surface element. Each discretised element is under the effect of a wrench due to solid-fluid interaction forces. The wrench on each element is a combination of the drag and the lift force acting on each element. We use volumetric element for a Frisbee but surface elements for the balls of all sizes. The use of volumetric elements is preferred over surface elements in Frisbee because it is known that a Frisbee experiences additional lift force due to the pressure difference above and below its surface. Each volumetric element has its own local velocity written in the world fixed frame  $\{G\}$ . The volumetric elements experience lift force due to varied air velocities on the top and the bottom surface. The boundary volumetric elements experience Magnus force for an additional side surface is exposed to air (Figure 1(a)). For surface elements, the lift generated by the Magnus force is the effective non-drag force, as only one surface is exposed to air (Figure 1(b)). The net wrench acting on the rigid body is the sum of all the wrenches acting on each element reduced to the centre of mass of the body.

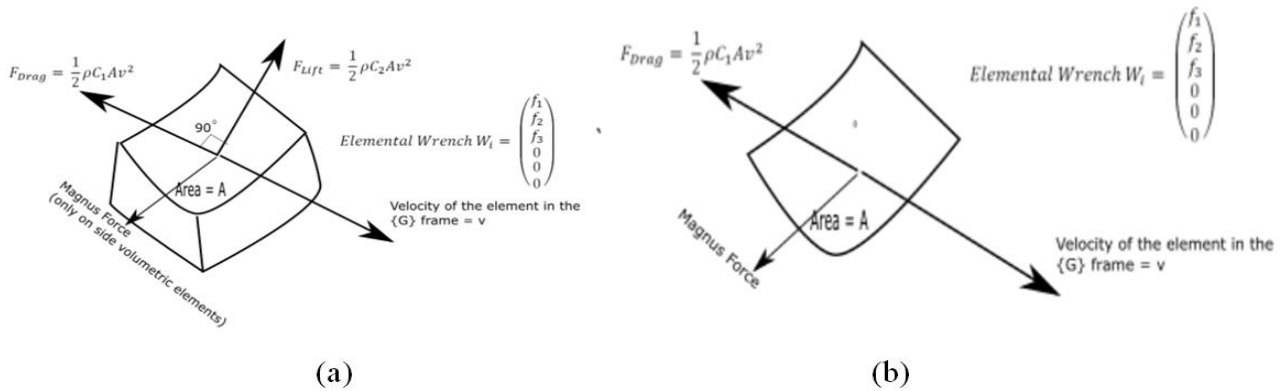


Figure 1: (a) Elemental forces on boundary (side) volume element of Frisbee (no side force for non-boundary elements); (b) Elemental forces on surface element of balls.

Throughout the complete analysis, unless specified otherwise, the pitch angle is defined as the angle made by the longitudinal axis of the object (local x-axis) with respect to the global longitudinal axis (x-axis) and the global velocity is directed at pitch angle, unless specified otherwise. The velocity vector, unless specified is in the x-z plane at an angle equal to the pitch angle with respect to the x-axis (Figure 2).

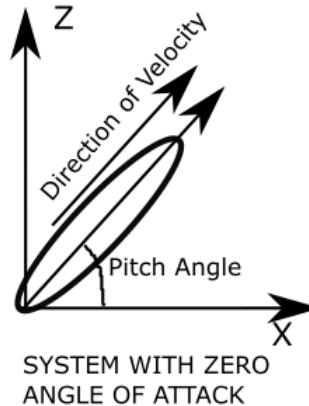


Figure 2: The object has zero angle of attack with velocity directed along the longitudinal axis in this paper unless specified other-wise (different for a Soccer Ball)

### 3 Analysis of a Frisbee

#### 3.1 Mathematical Prediction

The frisbee has been discretized into surface elements. The prismatic elements with small thickness aligned in a circle (Figure 3) is used to represent the Frisbee.

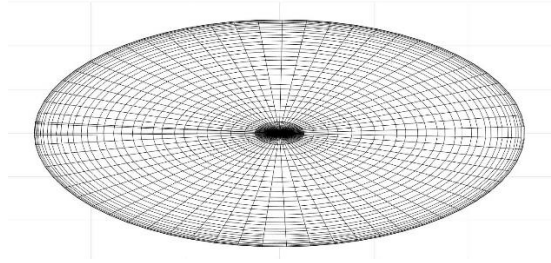


Figure 3: Discretisation of frisbee into prismatic elements top view shows the grid formation (1056 elements)

However, we hypothesize that the drag is a dissipative phenomenon and should be affecting the body locally rather than globally. The local wrench applied by the fluid force on the body should be analyzed in order to carry out subsequent prediction. The local wrench force applied on the body is as per the equation 1.

$$\vec{v}_{ele} = \vec{v}_o + \vec{\omega} \times \vec{r}_{eo} \quad (1)$$

All the terms in equation 1 are written with respect to the ground  $\{G\}$  frame. The magnitude of the elemental drag force (wrench of zero pitch is given in the equation 2.  $\vec{v}_{ele}$  is the representative notation to suggest the velocity of the centroid of an element.  $\vec{\omega}$  is the angular velocity of the body in the ground frame,  $\vec{r}_{eo}$  represents the radius vector joining the “e<sup>th</sup>” element to the centroid “O”. All the parameters are reduced to the earth fixed ground frame  $\{G\}$ .

$$W_{drag,ele} = \begin{pmatrix} -\frac{1}{2} \rho C_d \|v_{ele}\|^2 A_{ele} \hat{v}_{ele} \\ \vec{0} \end{pmatrix} \quad (2)$$

In the stated equation  $\rho$  is the density of air,  $C_d$  is the “elemental” coefficient of drag,  $A_{ele}$  is the area of the element under consideration. The drag force on the prismatic element acting locally will be due to the local velocity of the element. The lift force acting on each element is due to the pressure difference between the top and bottom surface. The local lift force shall be in the direction perpendicular to the local velocity of the object. Considering the fact that the lift force is never compressive or tensile, i.e. for a set of elements, it shall not be along the radius vector and it will always be perpendicular to velocity as that is the direction of maximum pressure difference, so the force should be also perpendicular to the radius vector of the element and the local velocity vector with respect to the center. All the vectors are represented in the earth fixed  $\{G\}$  frame.

The elemental lift force is given in the equations 3-4. The lift force is only characteristic to prismatic elements as the elements have a pressure difference between two surfaces. For pure surface elements, as single surface is exposed to atmosphere, the notion is evaded.

$$W_{drag,ele} = \begin{pmatrix} \vec{F}_{lift} \\ \vec{0} \end{pmatrix} \quad (3)$$

Accordingly, the lift forces are calculated as -

$$\vec{F}_{lift} = \begin{cases} \frac{1}{2} \rho C_l \|\vec{v}_{ele}\|^2 A_{ele} (\vec{v}_{ele} \times \vec{r}_{oe}) / \|\vec{v}_{ele} \times \vec{r}_{eo}\|, & \text{if } (\vec{v}_{ele} \times \vec{r}_{eo}) \cdot \hat{k} > 0 \\ \frac{1}{2} \rho C_l \|\vec{v}_{ele}\|^2 A_{ele} (\vec{r}_{oe} \times \vec{v}_{ele}) / \|\vec{v}_{ele} \times \vec{r}_{eo}\|, & \text{if } (\vec{v}_{ele} \times \vec{r}_{eo}) \cdot \hat{k} < 0 \end{cases} \quad (4)$$

" $\hat{k}$ " represents the unit vector aligned with the global z-axis (vertical axis). So, the net elemental wrench on the frisbee surface is given by the net reduction of the screws acting on the centroids of various elements. The wrench reduced to the center of the frisbee at any instance by combining the elemental lift and drag wrenches is given by the equation 5.

$$W_{sum} = \begin{pmatrix} \sum_{i=1}^n (\vec{F}_{drag,i} + \vec{F}_{lift,i}) \\ \sum_{i=1}^n (\vec{r}_{oi} \times \vec{F}_{drag,i} + \vec{r}_{oi} \times \vec{F}_{lift,i}) \end{pmatrix} \quad (5)$$

where  $\vec{F}_{drag,i}$  is the drag force on the  $i^{\text{th}}$  element,  $\vec{F}_{lift,i}$  is the lift force on the  $i^{\text{th}}$  element, " $\vec{r}_{oi}$ " is the radius vector from the centroid of the body to the center of the  $i^{\text{th}}$  element. The additional effect based on the body properties is the *Magnus Effect*. It is caused because of the pressure difference on the rotational surface of the body due to the angular velocities. The force is studied as an independent fluid force acting on the side surface of the prismatic element. The magnitude of the force is given by the equation 6.

$$\vec{F}_{magnus} = \rho C_m (2\pi r t) \|\vec{v}_o\|^2 (\vec{\omega} \times \vec{v}_o) / \|\vec{\omega} \times \vec{v}_o\| \quad (6)$$

Other coefficients might be available in the literature but constant scaling factors would be taken care by  $C_m$ . The magnus force for a spinning frisbee is because the whole body displaces the fluid. In equation 6,  $C_m$  is the magnus force coefficient, " $r$ " is the radius of the frisbee and " $t$ " is the mean thickness. The frisbee center of mass has a velocity vector  $\vec{v}_o$  and is spinning with the angular velocity  $\vec{\omega}$ .

The net external wrench acting on the rigid body (equation 7) undergoing motion is studied using forward dynamics. The predicted trajectory of the rigid body moving in atmosphere is given in the figures below. From the available known trajectories, the elemental  $C_d$  value was taken to be 0.03 and the  $C_l$  value was determined to be 0.085 from analysis of available trajectories of frisbee [1]. These coefficients are independent of the instantaneous angle of attack of the frisbee.

$$W_{net} = W_{sum} + \begin{pmatrix} \vec{F}_{magnus} \\ \vec{0} \end{pmatrix} \quad (7)$$

### 3.2 Simulation results

The result simulated was verified experimentally as well for two trajectory ranges. In the first case, the frisbee was simulated for the initial velocity of 7 m/s with the pitch angle of  $20^\circ$ . The angle of attack was kept to  $0^\circ$ . The mass of the frisbee is around 38 grams with the radius of 13 cm. The angular velocity initially imparted was around 108 rad/s. The frisbee was kept at the height of 1m. The predicted trajectory is shown in Figure 4.

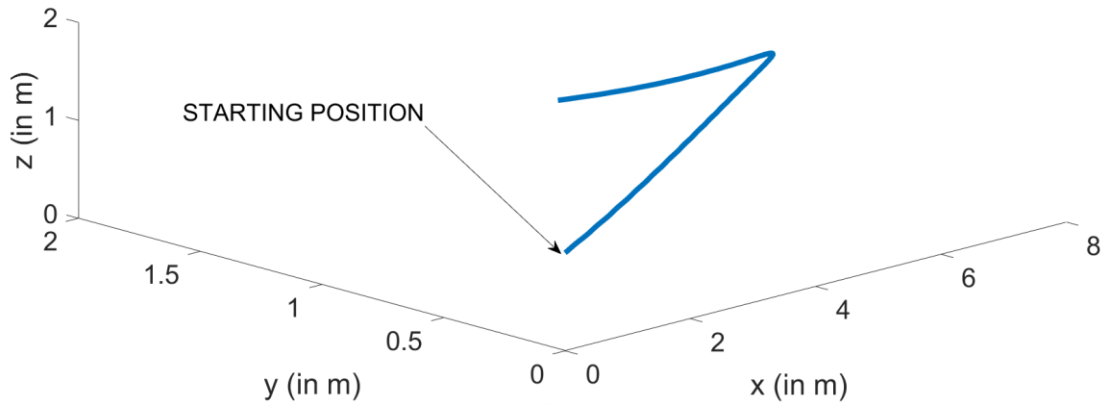


Figure 4: The skewed parabolic trajectory of the frisbee for the initial conditions stated above.

The time of flight predicted from the forward dynamics was around 1.88 s. The net range traversed by the frisbee was 7.47 m in the “x” direction (longitudinal) and 1.926 m in the “y” direction (lateral).

For another test case, the pitch angle of the frisbee was changed to  $11^\circ$  and the elevation was reduced to 3 cm. The predicted trajectory is shown in Figure 5.

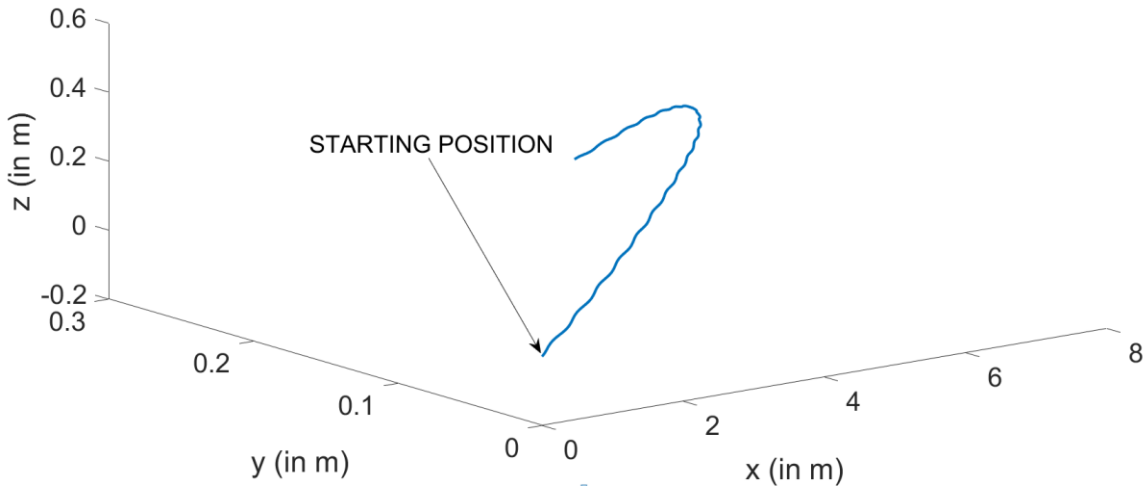


Figure 5: The skewed parabolic trajectory of the frisbee for the initial conditions stated above.

The trajectory time has reduced to 1.62 s, with the “x” direction range being around 7.18 m and the lateral range being around 0.59 m. The two trajectory ranges were being compared with the experimental results.

### 3.3 Experimental Setup

In order to verify the predicted range of the frisbee under a set of known initial conditions, an experimental setup was put up. The setup is presented in Figure 6.

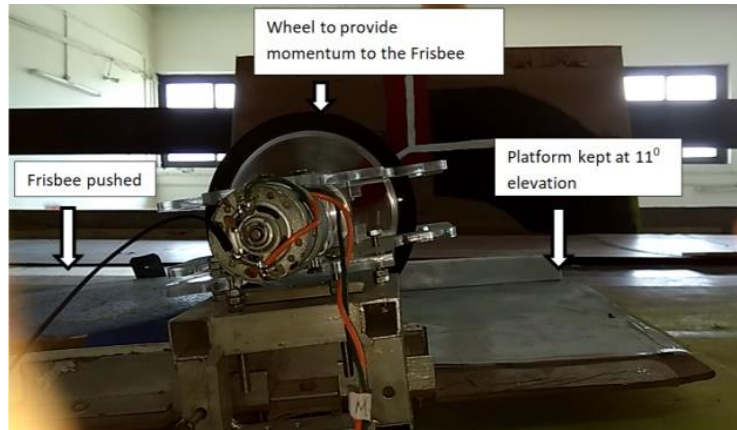


Figure 6: Experimental Setup to verify the simulated trajectories of the frisbee

The setup included a 12 V DC motor with velocity control connected to a wheel which is supposed to interact with the frisbee in a perpendicular manner. The interception of the wheel with the frisbee occurs at an offset so that the same input is able to give both the longitudinal velocity to the frisbee as well as the angular velocity. The velocity of the frisbee is predicted using vision techniques using a camera recording at around 27 fps. The angular velocity is predicted using basic kinematics. With various experimentation, the net results of the final range are as shown in Table 1 compared with the simulation result.

Table 1: Comparison of simulation results with experiments for frisbee (x-Longitudinal Deflection and y – lateral deflection at the end of the trajectory, NA – Not Available)

SN	Object	Details	Simulation (m)		Experimental (m) (8 tests performed)	
			x	y	x	y
1	Frisbee	Angle of attack = $0^{\circ}$ , Pitch = $11^{\circ}$ , $V= 7\text{m/s}$ , $\Omega = 108 \text{ rad/s}$	6.3	0.2841	7.3-8	0.35-0.8
2	Frisbee	Angle of attack= $0^{\circ}$ , Pitch= $20^{\circ}$ , $V= 7\text{m/s}$ , $\Omega=108 \text{ rad/s}$ thrown at Height= 1 m	7.472	1.926	Average 9 m	Average 2 m

It is observed that the simulated trajectories and the experimental trajectory ranges abide quite well to each other.

#### 4 Analysis of a Rugby Ball

The rugby ball is more like an ellipsoid with a major and a minor axis. The rugby ball is modelled using the surface elements' discretization (Figure 7).

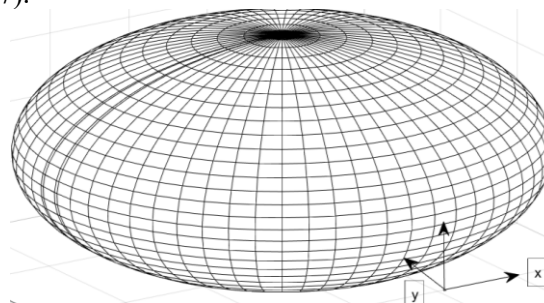


Figure 7: Surface element discretization for a rugby ball with the long axis being along the x-axis (2112 elements)

Any of the regular closed surface can be represented as a super ellipsoid [7]. The surface elements on the rugby ball experience the drag force due to the relative velocity of the surface element with the fluid. The body force

caused due to the magnus effect result in a force perpendicular to the angular and the linear velocity of the object. For the surface elements, the magnus coefficient value used is 0.31 and the elemental drag coefficient value is 0.1. The same elemental values are used for other bodies using surface elements in the same environmental conditions. The net magnus force on each element is given in the equation 8. The magnus force depends on the net area of each of the surface added together. The force is given in the equation 8, where ( $A_{surface}$ ) is the net surface area of the ellipsoid or any other rigid body modeled as surface elements.

$$\vec{F}_{magnus} = \rho C_m (A_{surface}) \|\vec{v}_o\|^2 (\vec{\omega} \times \vec{v}_o) / \|\vec{\omega} \times \vec{v}_o\| \quad (8)$$

Other scaled formulation of magnus force might be available in the literature but constant scaling factors would be taken care by  $C_m$ , once identified. The net reduced wrenches to the centroid of the object is given in equation 9.

$$W_{sum} = \begin{pmatrix} \sum_{i=1}^n (\vec{F}_{drag,i}) + \vec{F}_{magnus} \\ \sum_{i=1}^n (\vec{r}_{oi} \times \vec{F}_{drag,i}) \end{pmatrix} \quad (9)$$

The magnus force doesn't lead to additional moment as it is symmetric with respect to the centroid. The combination of forces is reduced to the center of the object. The trajectory is predicted using the forward dynamics. For both the trajectories, the mass of the rugby ball is taken to be 430 grams and the long axis being of size 14.5 cm and the short axis of 9.55 cm.

The trajectory of the rugby ball was simulated for a case of two particular techniques available in the literature of sport, i.e the punt kick and the screw kick. Each of this has specific angular velocity direction and the longitudinal motion. In the screw kick case the ball rotates about its long axis where as in the punt case the ball is made to rotate about its short axis. To simulate the punt kick, the ball was given an initial velocity of 23 m/s and is rotated about the y-axis at 62.8 rad/s. The initial pitch angle is around  $55^\circ$  and the rugby ball is at 0 m elevation from the ground. The simulated trajectory is shown in Figure 8.

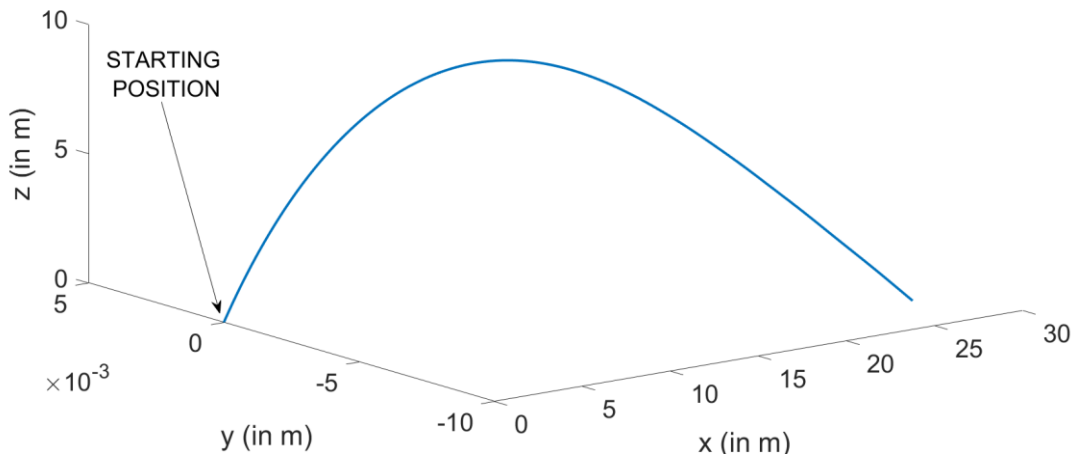


Figure 8: The trajectory of the rugby ball simulated under punt kick.

Under the screw kick, the object is made to rotate about the long axis (x-axis). The initial velocity given is around 28 m/s with the angular velocity of 45 rad/s and the initial pitch angle of around  $35^\circ$ . The simulated trajectory is shown in Figure 9.

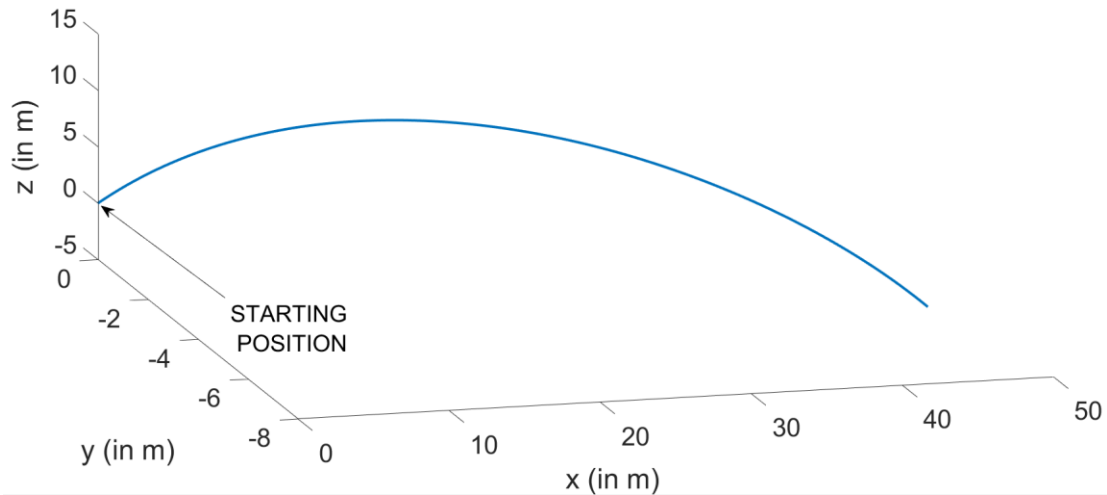


Figure 9: The trajectory of the rugby ball simulated under screw kick. The initial conditions are stated above.

The analysis in [3] shows the experimental range of the rugby ball for the specified set of the motion coefficients. It can be observed that the systems adhere well. The comparison between the experimental and the simulated results are shown in Table 2.

Table 2: Comparison of simulation results with experiments for rugby ball (x-Longitudinal Deflection and y – lateral deflection at the end of the trajectory, NA – Not Available)

SN	Object	Details	Simulation (m)		Experimental (m)	
			x	y	x	y
1	Rugby Ball	Screw Kick, linear velocity = 28 m/s, Angular Velocity = 45 rad/s, Pitch = 35 <sup>0</sup>	43.27	7.037	35-47	-3.7-7.5
2	Rugby Ball	Punt Kick, linear velocity = 23 m/s, Angular Velocity = 62.8 rad/s, Pitch = 55 <sup>0</sup>	27.27	-0.007	28-35	-1.1-6.3

## 5 Analysis of a Tennis Ball and a Soccer Ball

Tennis ball and Soccer Ball are both spherical in nature. It is also analyzed using a set of surface elements as in rugby ball. The surface elements again are a combination of drag forces and the body magnus forces. The net individual forces acting on each of the surface reduced to the center of the ball results in the net wrench based on the set of surface elements. The reduction of the elemental surface wrenches is exactly similar to that used in rugby ball. The same surface coefficients are used as in the case of a rugby ball for both football and the soccer ball (equation 8 and 9).

### 5.1 Results for a Tennis Ball

The trajectories for a tennis ball has been simulated for two cases, one with a top spin, where the ball is given a rotational velocity about the vertical axis. The simulated trajectory for a spherical tennis ball of mass 36 grams and radius 3.6 cm. The initial velocity for simulation is 30 m/s with top spin of 125 rad/s. The initial elevation in the vertical axis is 1 m. The trajectory of the tennis ball is shown in Figure 10. The pitch angle is 5.5<sup>0</sup>.

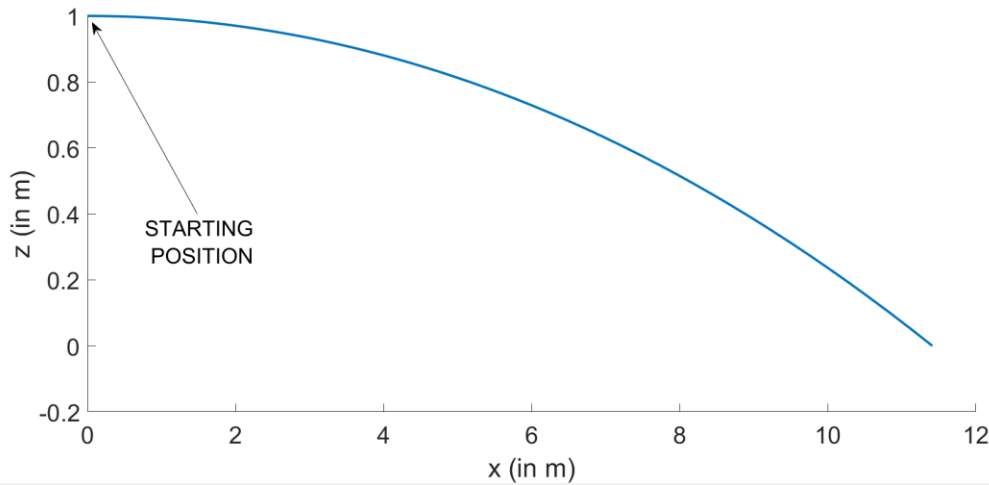


Figure 10: The trajectory of the tennis ball simulated under top spin. The x-z motion is shown as the lateral y-motion had negligible ranges (around  $10^{-4}$  m). The x and z trajectories are in meters.

The direct motion of the tennis ball without any lateral motion is also simulated, the linear velocity is 30 m/s with no top spin. The trajectory simulated is presented in Figure 11.

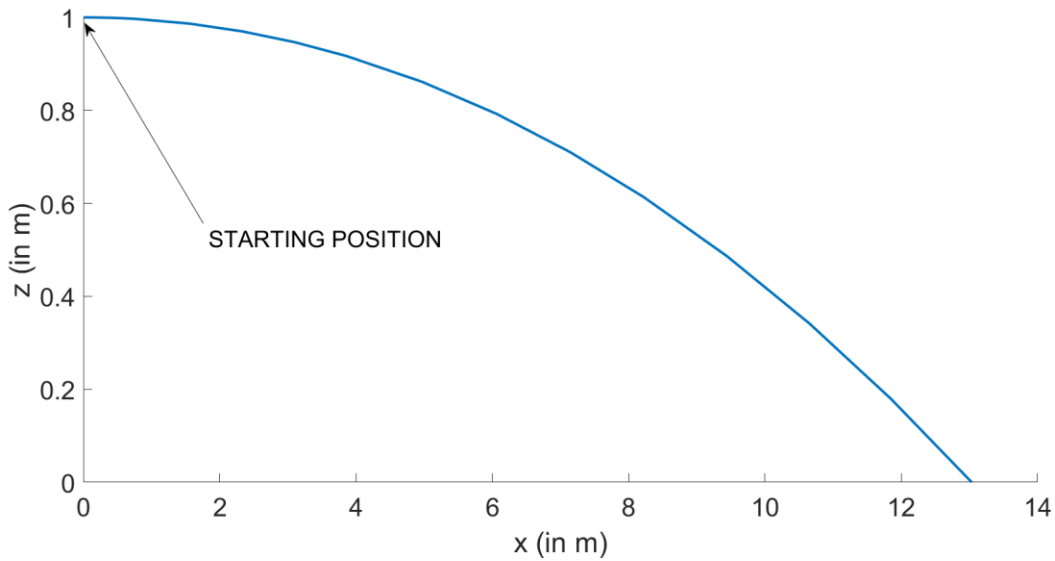


Figure 11: The trajectory of the tennis ball simulated without any spin. The x-z motion is shown as the lateral y-motion had negligible ranges (around  $10^{-4}$  m).

The experimental trajectories for the same initial conditions are presented in [4]. The comparison of the simulated trajectory with the experimental trajectory is presented in Table 3.

Table 3: Comparison of simulation results with experiments for rugby ball (x-Longitudinal Deflection , NA – Not Available)

SN	Object	Details	Simulation (x – in m)	Experimental (x - in m)
1	Tennis Ball	With top spin of 20 rev/s (Velocity = 30 m/s, Elevation = $5.5^0$ )	11.43	10.85
2	Tennis Ball	No spin (V=30 m/s, Elevation= $5.5^0$ )	13.03	12.86

The simulation results quite well adhere to the experimental results (Table 3). It is observed that the presence of the top spin forces the ball to fall early in the tennis court, which makes it a nice maneuver to the player.

### 5.2 Results for a Soccer Ball

The soccer ball is again modeled with surface elements with the same equations as that of a rugby ball (and same force coefficients as well). The trajectory is simulated for a pitch angle of  $45^{\circ}$  and unlike the previous cases, the velocity component on the ground is directed along a vector making an angle of  $38^{\circ}$  with the x-axis. So, unlike the previous cases, here the initial y-component of the velocity is not zero. The magnitude of angular velocity is 88 rad/s with respect to the vertical axis. The mass of the football is taken to be 412.4 grams with a radius of 11 cm. The initial height is 0 m. The simulated trajectory for the given set of case is shown in Figure 12.

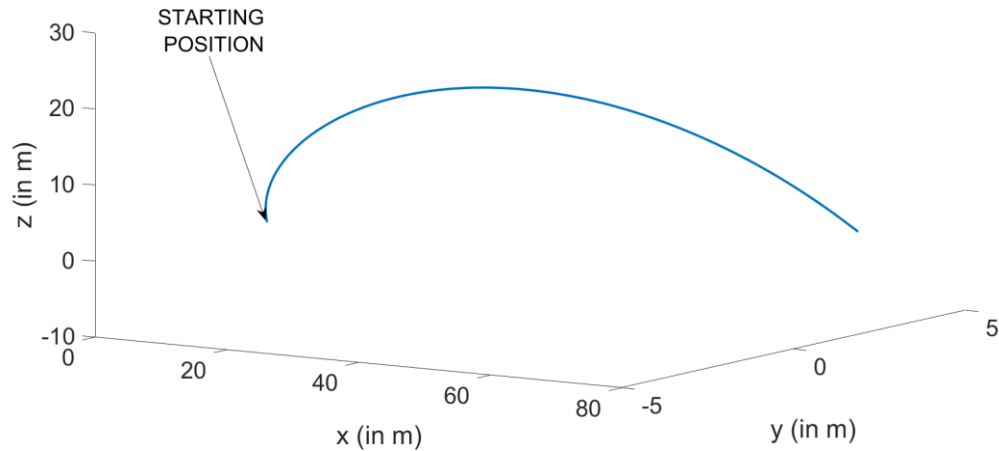


Figure 12: The trajectory of the football simulated with components of velocity in all the three directions

The comparison of the interception of the goal post (the case presented) [5] with respect to the experimental analysis is presented in Table 4. The goal post is at the longitudinal distance of 35 m. So, the deflection of the football was in the x-y plane needed to be less than 2.42 m if it had to enter the goal post. So, the deflection of the football from the simulated trajectory when  $x = 35$  m is compared (Table 4).

Table 4: Comparison of simulation results with experiments for football (x-Longitudinal Deflection and y – lateral deflection at the end of the trajectory, NA – Not Available)

SN	Object	Details	Simulation (m)		Experimental (m)	
			x	y	x	y
1	Football	Y deflection at 35 m X deflection for $V = 38$ m/s and ground angle = $12^{\circ}$ and Vertical Angle = $45^{\circ}$	-	1.75	-	2.42

## 6 Conclusions

This paper presents a methodology to predict the trajectory of motion of sports' object moving in a space. The prediction is based on interaction of fluids with the rigid bodies based on finite element discretizations. It is claimed that the concepts of drag force is a local phenomenon. So only the local velocity of the object should affect the motion. Additionally, it is claimed that the true coefficient of drag force should be independent of the net surface of the object and should just be dependent on the type of the element. Two types of elements are developed, frisbee is modeled with prismatic elements and other sports utilities such as rugby ball, tennis ball and soccer ball are modeled with surface elements. Both the elemental forces and the body forces are reduced to get the final wrench describing the motion of the object after putting in forward dynamics. The results for frisbee were experimentally verified and for other utilities, results were matched with the available literature. The elemental coefficients were

developed and used with multiple objects. The elemental force coefficients are proved to be invariant to the shape of the object for surface elements. For prismatic elements, the trajectories were matched with experimental results and the elemental method gives the same “*skewed parabolic*” trajectory as that available in the literature.

## Acknowledgements

We acknowledge the help of Robotics Club, Indian Institute of Technology Delhi, India to help us in performing the experimental verification of the range of the frisbee. We also acknowledge the help of Dr. Amit Gupta, Associate Professor, Indian Institute of Technology Delhi, India for his insight in the field of fluid dynamics that has helped us a lot.

## References

- [1] Hummel SA. (2003) Frisbee flight simulation and throw biomechanics. University of California, Davis.
- [2] Crowther, W. J., & Potts, J. R. Simulation of a spin-stabilised sports disc. *Sports Engineering*, 10(1), 3-21
- [3] Suito, H. (2009). Computational analysis for motions of rugby balls interacting with air flows. *Football Science*, 6, 34-38.
- [4] Cross, R. (2002). Measurements of the horizontal coefficient of restitution for a superball and a tennis ball. *American Journal of Physics*, 70(5), 482-489.
- [5] Bush JW. (2013), The aerodynamics of the beautiful game, Department of Mathematics, MIT.
- [6] Kang S, Choi H, Lee S. (1999) Laminar flow past a rotating circular cylinder. *Physics of Fluids*. Nov;11(11):3312-21.
- [7] Knill, Oliver. The Super Eggs and Other Super Surfaces. 2009. [http://www.math.harvard.edu/archive/21a\\_fall\\_09/exhibits/superegg/](http://www.math.harvard.edu/archive/21a_fall_09/exhibits/superegg/) (accessed March 2, 2017).